African Journal of Biotechnology Vol. 10(75), pp. 17223-17240, 28 November, 2011
Available online at http://www.academicjournals.org/AJB
DOI: 10.5897/AJB11.3050
ISSN 1684–5315 © 2011 Academic Journals

Full Length Research Paper

Hydrogeochemical and hydrogeological investigations of thermal waters in the Alasehir-Kavaklidere area (Manisa-Turkey)

Ali Bülbül*, Tuğbanur Özen and Gültekin Tarcan

[1]Pamukkale University, Department of geological Engineering, Denizli, TURKEY.
[2]Dokuz Eylül University, Department of geological Engineering, İzmir, TURKEY.

Accepted 29 August, 2011

Alasehir graben is located in the southern edge of the Gediz graben, which is an important graben for geothermal activity. Thermal waters are hosted by Menderes massif metamorphic rocks, which are made of gneisses, schists and marbles. Impermeable clayey units of the neogene sediments are cap rocks of the geothermal system. Presence of geothermal waters is closely related to normal fault systems and graben tectonic. Meteoric waters recharging the reservoir rocks are heated at depth with geothermal gradient. The AK-2 and KG-1 wells have the third and fourth highest temperatures of Turkey, respectively. Reservoir temperatures of the geothermal system are estimated to vary between 125 and 225°C by mineral equilibria geothermometer, vary between 160 and 240°C by Giggenbach triangular diagram and vary between 150 and 250°C by silica enthalpy-mixture model. Cold water contributions to thermal waters vary from 75 to 95%. Na-HCO_3 water type is dominant for thermal water. Major reaction of the thermal water to change facies is softening reaction. The temperatures obtained from silica enthalpy model, mineral equalibria geothermometers, Na/K, Na/Li geothermometers are more useful than others in the study area. Scaling tendencies of the thermal water are examined. The major environmental problem in the groundwater is high boron concentration which is harmful for agricultural irrigation.

Key words: Alasehir, geothermal systems, hydrogeochemistry, saturation index, geothermometer.

INTRODUCTION

Alasehir-Kavaklidere area is one of the most important geothermal fields of Turkey (Figures 1, 2 and 3) that is located in southern part of the Gediz graben in western Turkey. Because of faults, Alasehir had some important earthquakes. Its climate is arid and dry in summers. Annual mean precipitation is approximately 500 mm/year. Stock-breeding, grapery, olive growing, fruit growing, cotton and tobacco growing, many factories and greenhouses, support economic activity. Avsar dam, the nearest dam to the county, is important for irrigation in the region. The groundwater of the plain has some qualification problems for utilization. There are many wells in alluvium, but some of them are not suitable for irrigation or drinking because of high boron and sodium concentrations (Bülbül, 2009). The study area is famous for agricultural soils, archaeological sites and natural beauties. Grape production of the area is significant in Turkey (Figures 1 and 2). This paper focuses on geothermometer applications and conceptual geothermal model in the study area, scaling tendencies of the thermal waters and high boron concentration in the thermal water.

*Corresponding author. E-mail: abulbul@pau.edu.tr. Tel: +90 258 296 34 01. Fax: +90 258 296 33 82.

MATERIALS AND METHODS

Water samples of springs and wells were collected in September 2007. Conductivity (EC), pH and temperature were measured in the field using standard hand-held calibrated field meters. Water samples were analyzed for their chemical (major ion) compositions by inductively coupled plasma–mass spectrometer (ICP–MS) in the ACME Laboratories in Canada. Total alkalinity was measured by

Figure 1. A view of Alasehir plain.

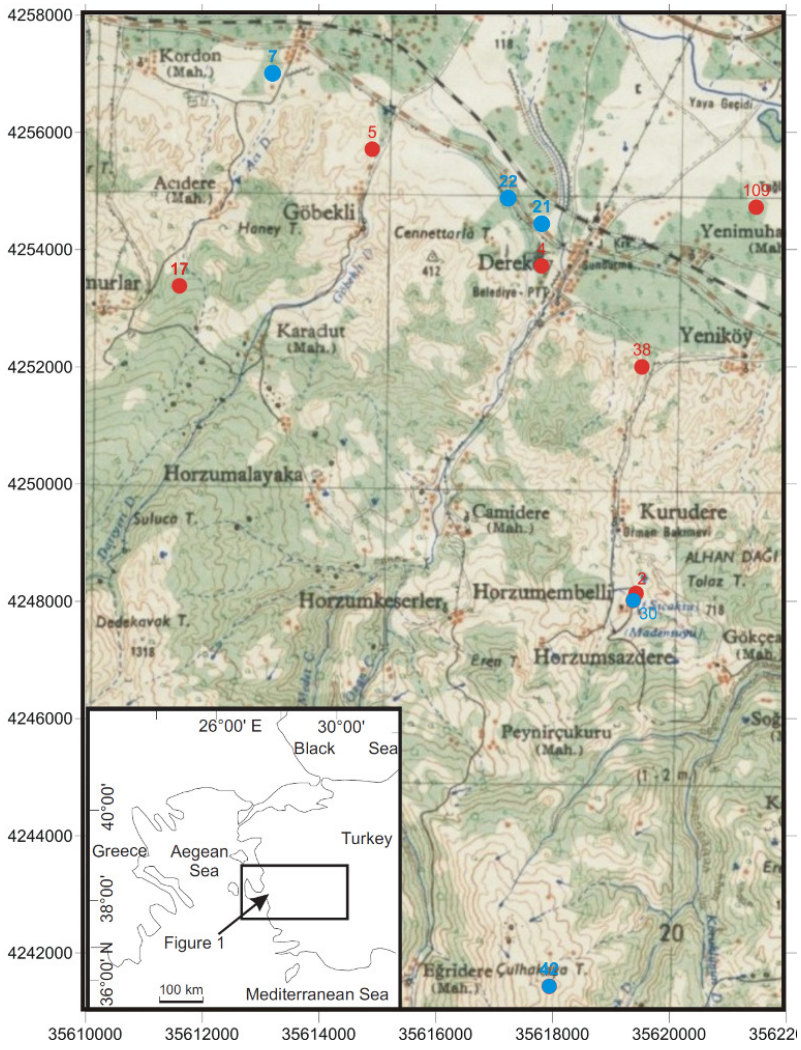

Figure 2. Location of study area and water samples map.

titration with Nitric acid to a final pH of 4.2. SO_4 was analyzed by means of gravimetric precipitation method in Geochemistry Laboratories from Department of Geological Engineering in Dokuz Eylul University. AQUACHEM (Calmbach, 1997) and PhreeqC-2.11 (Parkhurst and Appelo, 1999) software were used to plot the diagrams and calculate the saturation index. Also EXCEL-2003

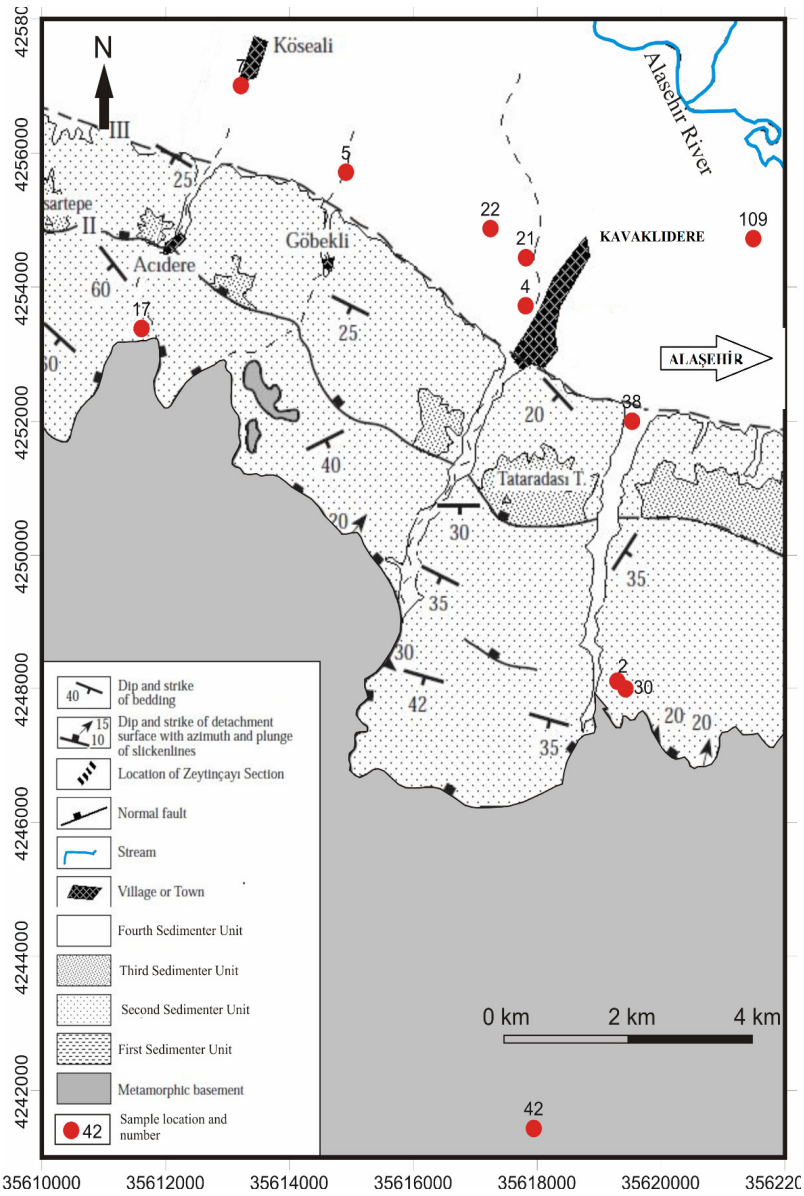

Figure 3. Geological map and water samples (Seyitoglu et al., 2002).

was used to estimate reservoir temperature by means of geothermometer formulas.

Geological settings

The Alasehir graben is situated in the Western Anatolian extensional province (Dewey and Sengor, 1979). Both the southern and northern margins of the Alasehir graben are dominated by non-marine sediments that show marked lateral and vertical facies variation (Purvis and Robertson, 2005). The graben fill is composed of four sedimentary units. The first sedimentary unit is the lowermost part of the graben fill. The formation unconformably overlies the metamorphic basement south of the town of Alasehir and its base is comprised of very angular boulder conglomerates containing schists, metagranites, porphyritic gneisses and mylonitic augen gneisses. The formation continues with alternating yellowish sandstone and mudstone. The overall sedimentary sequence of the lower part of the Alasehir formation exhibits a fining-upwards character within a short vertical distance of nearly 50 m. Intervals of 1.5 m thick, very angular boulder conglomerate are common in the fine-grained lacustrine sediments. The uppermost part of the formation is composed of dominantly organic-rich, very well-lithified, laminated mudstone which gradually passes upwards into sandstones with limestone layers and conglomerates. The Alasehir formation is conformably overlain by the second sedimentary unit. The second sedimentary unit has a dominant red colour (Seyitoglu and Scott, 1996a). Its lowermost part is a dark red angular conglomerate. Upper levels, however, are composed of alternating light red- and grey-coloured conglomerate and sandstone.

The lower to middle Miocene first and second sedimentary units are unconformably overlain by the third sedimentary unit that consists of light yellow semi-lithified conglomerates and sandstones (Seyitoglu and Scott, 1996a) of Pliocene age. The fourth sedimentary unit comprises recent alluvium deposits (Figure 3) (Seyitoglu et al., 2002).

RESULTS

Hydrogeological settings and geothermal system

Alluvium aquifer is determined as the 4th sedimentary sequence. It is unconfined and hosts cold groundwater. Therefore there are many irrigation wells with variable depths in the alluvium aquifer. Also there is a confined aquifer, which is metamorphic basement hosting thermal water. General flow path of groundwater is from south to north. Alasehir stream derives surface water to Gediz river. Thermal waters are hosted by marbles and fractured Menderes massif rocks that consist of gneiss, schist and quartz. Cap rock of the geothermal system is an impermeable clayey level of neogene sediments. Thermal waters have meteoric origin. There are thermal waters that are heated at depth due to geothermal gradient (Figure 4). So there are many thermal spas and thermal drills. They are Horzumsazdere thermal Spa (number 2), (Figure 5), Horzumsazdere mineral water Spa (number 30) and Acidere Turtle Spa (number 17). There are four thermal deep drills in the area. The AK-2 (213°C) and KG-1 (182°C) (Figure 6) thermal drills were drilled by MTA. These wells have the third and fourth highest downhole temperatures of Turkey. KG-1 (number 5) and AK-2 (number 38) have 1447 and 1501 m depths, respectively (MTA, 2005). The production quantity of KG-1 well is tested as 12 l/s (Karahan et all, 2003). In addition, AK1 (number 4, 63°C downhole temperature) (Figure 7) drill and number 109 well (greenhouse drill) have depths of 750 and 700 m, respectively KG-1 drill has an electrical conductivity of 5690 µS/cm which is the maximum value among all of the wells (Table 1).

Number 42 is a cold water Spa ascending in the recharge area with high topographic elevation (1400 m) and it is used as cold water recharge point for silica enthalpy diagrams and silica mixing models. Also there are many wells (number 7, 21 and 22) for irrigation whose waters are mixed with thermal waters by means of graben fault in alluvium aquifer.

Hydrogeochemistry and geothermometers

$Na\text{-}HCO_3$ water type is dominant for thermal water. Also $Na\text{-}Mg\text{-}HCO_3$, $Ca\text{-}Na\text{-}HCO_3$ water types occur in the study area and thermal waters have very high boron concentration (max: 124 ppm). Source of boron can be evaporites and carbonates due to the high correlation between B-Na, B-Cl, $B\text{-}HCO_3$ and $B\text{-}SiO_2$ in the correlation matrix table (Table 2, Figure 10a, b, c and e), Boron in thermal waters is also probably controlled by the contribution of B by degassing of magma intrusives. Also Sericite, Illite and Tourmaline minerals, which are abundant in Menderes Massif rocks, are considered to be main reason for the high boron concentration (Gemici and Tarcan, 2002). Cl-EC diagram (Figure 10h) and correlation matrix $EC\text{-}HCO_3$, EC-B (Table 2) show that all thermal waters have deep circulation and meteoric origin. In addition, isotope data show that thermal waters are older than 50 years so Alasehir-Kavaklidere geothermal system has a deep circulation system and all of the waters have meteoric origin (Bülbül, 2009). The thermal waters have high B/Cl ratios so Kavaklidere-Alasehir geothermal system is a young system (Bülbül, 2009). Giggenbach diagram shows that water rock interaction has not finished and most of the waters are immature waters. Three of them are partially equilibrated waters (Figure 8). In order to estimate the reservoir temperature many geothermometers were applicated (Tables 3, 4 and 5). Reservoir temperatures of the geothermal systems are estimated to vary between 160 and 240°C by Giggenbach triangular diagram (Figure 8). The temperature estimated by silica mixing model varies between 150 and 250°C (Figure 12). Cold water contribution to thermal water varies from 75 to 95%. The reservoir rock temperature is estimated as 232°C by silica enthalpy model (Figure 11). The silica enthalpy model, the mineral equilibria geothermometers and Na/K and Na/Li geothermometers are more useful than other geothermometers in the study area. Also saturation index conductive cooling mineral equilibria diagrams are used to estimate the temperature of reservoir rocks. When the most of the minerals have intersection point near SI = 0 line, the point shows the temperature of geothermal system (Reed and Spycher, 1984). So reservoir temperatures of the geothermal systems are estimated to vary between 125 and 225°C by mineral equilibria geothermometer (Figure 13).

Cold waters generally have $Ca\text{-}HCO_3$, $Ca\text{-}Mg\text{-}HCO_3$ water facies because of dissolution of carbonates (Tables 1 and 2; Figure 10d and g). Clayey levels of schists at the flow path of thermal waters cause natural softening reaction during the geochemical evolution of groundwater because of Ca and Mg ions exchange with Na and K ions. So Ca-Mg-HCO3 and Ca-HCO3 water types convert to Na-HCO3 and Na-Ca-HCO3 water types. Softening reaction is one of the most important reactions for evolution of thermal waters (Figure 9). Because of degassing magma intrusives, AK-1 has high SO_4 (280 mg/l) and H_2S (2.5 mg/l) concentrations (Bulbul, 2009).

Saturation index and scaling tendencies

Saturation index (SI), which is the degree of saturation of a particular mineral in an aqueous solution, can be obtained from its solubility product and its reaction quotient (activity product):

$$SI = \log Q - \log K = \log (Q/K)$$

Where Q is the calculated activity product and K is equilibrium constant (Gökgöz, 1998). It indicates scaling

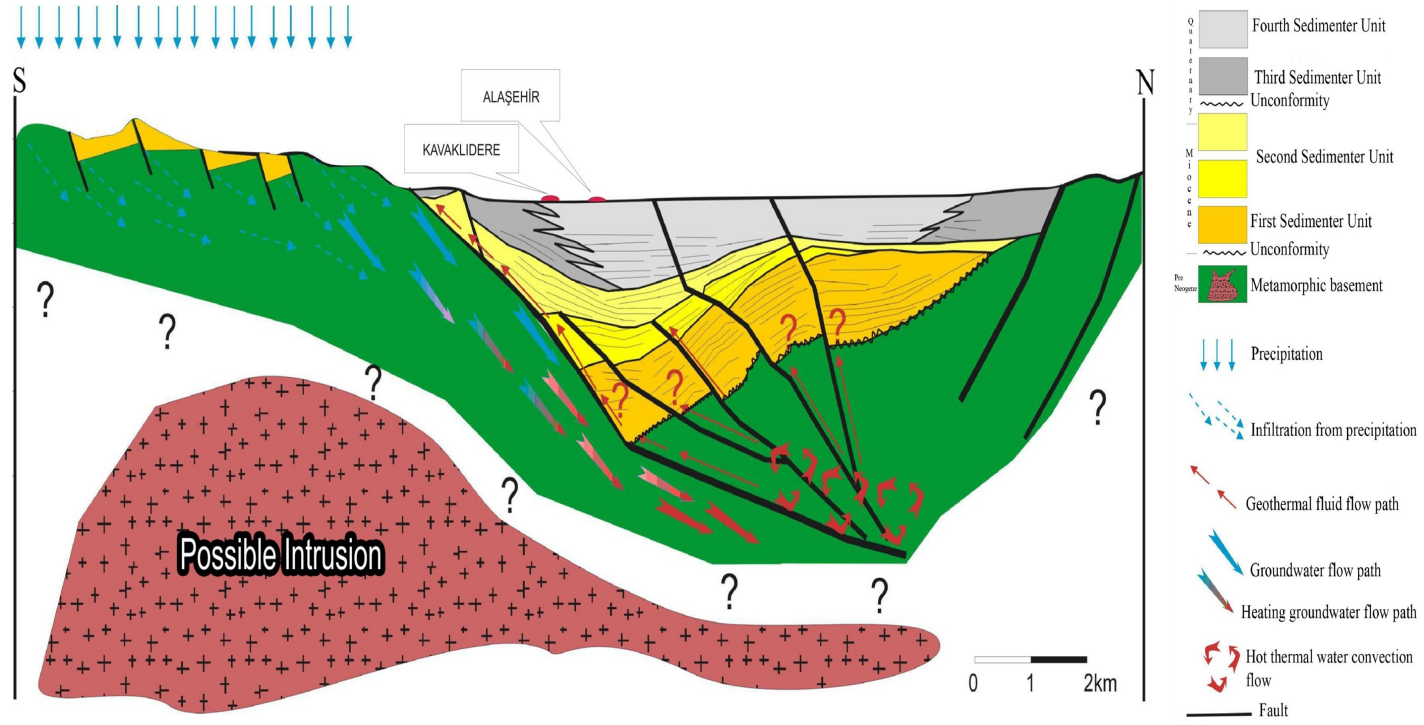

Figure 4. Conceptual geothermal model (Çiftçi and Bozkurt, 2009).

Figure 5. A view of Horzum Sazdere spa (sample 2).

Figure 6. A view of KG - 1 drill (sample 5).

Figure 7. A view of AK -1 drill (Sample 4).

and solubility tendencies of any mineral in any fluid at outlet temperatures.

Tendencies of the thermal water are examined. At the outlet temperature, aragonite, k-feldspar, k-mica, quartz, amorphous silica, dolomite, calcite, barite, gibbsite, goethite, hematite and talc have precipitation tendencies. Alunite, anorthite, anhydrite, gypsum, manganite, rhodocrosite, sepiolite, siderite, strontionite and witherite tend to solve. Some of the minerals might have scaling problems in the well and pipes. They are calcite, aragonite, dolomite, quartz and amorphous silica (Table 6, Figures 13 and 14).

DISCUSSION AND CONCLUSION

Thermal waters are hosted by Menderes Massif metamorphic rocks which consist of gneisses, schists and

Table 1. Physical measurements and chemical analyses of the water samples from Alasehir and Kavaklidere geotermal areas. T (°C): Values are measured as outlet temperatures (deep well temperatures; *63°C, **183°C and ***213°C). pH: standard unit at 25°C , EC: electrical conductivity (µS/cm).

Site	2	4	5	7	17	21	22	30	38	42
	Horzum Sazdere spa	AK-1 (MTA deep drill)	KG-1 (MTA deep drill)	Koseali town well	Acidere spa	Well (at Kavaklidere)	The well between Kavaklidere Koseali	Horzum Sazdere spa	AK-2 (MTA deep drill)	Culhakaya Hill spa
Date	16-02-2007	02-03-2007	02-03-2007	22-02-2007	08-05-2005	02-03-2007	02-03-2007	08-05-2005	08-05-2005	08-05-2005
pH	6.58	8.14	6.38	7.34	6.06	6.54	6	8.34	7.99	7.94
Eh (mV)	170	0	22	22	42	14	27	-90	-72	-68
T (°C)	30.6	21*	23**	24.4	29.1	28	31	16.7	45***	24.4
EC(µS/cm)	3720	4450	5480	720	1735	1445	1655	2240	3150	203
Na	715.0	1289.7	1718.4	79.8	186.1	201.3	236.4	307.3	926.0	19.3
K	66.9	17.6	58.9	6.2	11.9	6.8	8.3	43.3	103.5	3.8
Ca	116.6	5.0	11.9	42.4	191.2	97.7	130.4	39.5	10.8	25.7
Mg	65.3	1.8	2.2	19.1	30.5	48.8	47.0	118.9	1.4	10.3
HCO_3	2563	2929	4424	330	1210	992	1007	917	2055	78
Cl	169	342	174	33	22	28	38	86	224	8
SO_4	25	280	31	51	6	42	51	138	48	21
SiO_2	181.7	89.7	201.2	31.2	88.3	58.8	47.8	55.4	491.9	16.5
B	110.56	15.00	107.59	1.01	8.19	3.45	2.17	41.58	124.14	0.31
Fe	0.000	10.39	68.57	0.06	2.45	0.14	0.07	0.00	1.07	0.34
Li	6.34	0.63	3.70	0.07	0.33	0.09	0.06	2.15	7.72	0.01
Al	0.05	0.53	0.14	0.03	0.03	0.01	0.00	0.00	0.43	0.33
As	0	0.26	0	0.005	0.001	0.002	0.001	0.011	0.79	0.004
Mn	0.28	0.04	1.20	0.006	0.58	1.21	0.26	0.00	0.02	0.022
Water type	Na-HCO_3	Na-HCO_3	Na-HCO_3	Na-Ca-Mg-HCO_3	Ca-Na-HCO_3	Na-Ca-Mg HCO_3	Na-Ca-HCO_3	Na-Mg-HCO_3	Na-HCO_3	Ca-Mg-Na-HCO_3

Presence of geothermal waters is closely related to normal fault systems and graben tectonic. As the aquifer system hosting the geothermal fluids is confined, the geothermal fluids ascend throughout the detachment fault that is located in the south of the graben. Meteoric waters recharging the reservoir rocks are heated at depth with geothermal gradient (Figure 4). Cold waters generally have Ca-HCO_3, Ca-Mg-HCO_3 water facies because of dissolution of carbonates. Clayey levels of schists at the evolution path of thermal water causes natural softening reaction. So Ca and Mg ion exchanges Na and K ions. Softening is one of the most important reactions in the evolution of thermal waters. The temperatures obtained from silica enthalpy model, mineral equalibria geothermometers, Na/K, Na/Li geothermometers are more useful than others in the study area. High boron concentration in thermal water and groundwater in alluvium aquifer is caused by the contribution of thermal water to cold groundwater. So groundwater loses qualification for utilizing in irrigation and drinking. Calcite, aragonite, dolomite, quartz and amorphous silica have scaling tendencies. In order to prevent scaling in pipes and wells, some kinds of inhibitors can be used. In order to keep the temperature of the system and to recharge the system, reenjection of thermal water is necessary during the operation of the system. So, environmental harmful impact of thermal water can be prevented. Also re-injection temperatures can be determined by means of

Table 2. Correlation matrix of some chemical and physical parameters for thermal waters in the study area.

	NA	CA	MG	CL	SO_4	Li	HCO_3	SiO_2	B	As	Br	Ba	Sr	Mn	K	Cond	T (Wa)
NA	1.0	-0.5	-0.4	0.8	0.4	0.2	1.0	0.5	0.6	0.7	0.7	0.6	0.3	0.2	0.6	1.0	0.2
CA		1.0	0.3	-0.5	-0.5	-0.1	-0.3	-0.3	-0.3	-0.4	-0.5	-0.4	0.5	0.2	-0.3	-0.3	0.1
MG			1.0	-0.3	0.0	0.1	-0.3	-0.3	-0.1	-0.4	-0.3	-0.5	0.3	-0.1	0.0	-0.2	-0.2
CL				1.0	0.6	0.5	0.7	0.5	0.5	0.4	1.0	0.7	0.0	-0.1	0.5	0.8	0.0
SO_4					1.0	-0.1	0.3	-0.1	-0.2	0.3	0.6	0.1	-0.3	-0.4	-0.1	0.4	-0.1
Li						1.0	0.2	0.8	0.8	0.4	0.5	0.7	0.2	-0.3	0.9	0.3	0.4
HCO_3							1.0	0.5	0.6	0.6	0.7	0.5	0.5	0.4	0.5	1.0	0.2
SiO_2								1.0	0.8	0.7	0.5	1.0	0.1	0.0	0.9	0.5	0.5
B									1.0	0.3	0.5	0.7	0.4	0.1	0.9	0.6	0.1
As										1.0	0.3	0.6	0.0	-0.3	0.5	0.6	0.9
Br											1.0	0.7	0.1	-0.1	0.5	0.8	0.0
Ba												1.0	0.0	-0.1	0.8	0.5	0.4
Sr													1.0	0.4	0.3	0.5	0.1
Mn														1.0	-0.1	0.2	-0.1
K															1.0	0.6	0.3
Cond																1.0	0.2
T(Wa)																	1.0

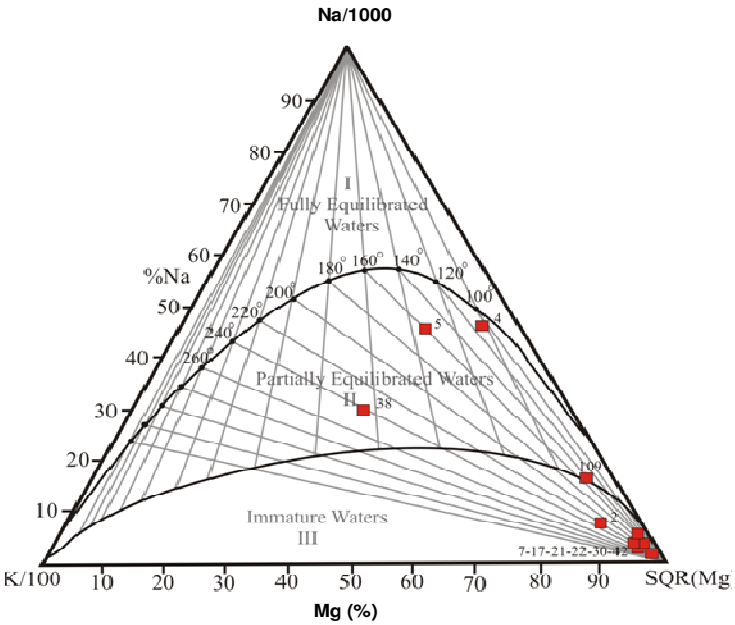

Figure 8. Distribution of the thermal waters from study area in the Na-K-$Mg^{1/2}$ triangular diagram (Giggenbach, 1988).

conductive cooling-mineral saturation index graphics. Re-injection temperature is suggested to be approximately 50 to 75°C (Figure 13). The estimated reservoir rock temperature is higher than 150°C, thus, according to Lindal diagram, Alasehir-Kavaklidere geothermal system is suitable for applications that use conventional power and for the purpose of space heating (buildings and greenhouses), Alumina via Bayers process, food caning, evaporation in sugar refining, drying of fish meal and timber, refrigeration, drying and curing of light aggregate cement slabs, mushroom growing and drying farm products (Figure 15).

In addition, this geothermal system is suitable for the production of dry ice from liquid carbondioxide economically. Two of the thermal waters in the study area [number 2 (Horzum Sazdere spa), number 5 (KG-1 well)]

Table 3. Chemical geothermometers formulas and references.

S/No	Geothermometers	Formulas	References
1	SiO_2 (Amorphous silica)	$t = 731 / (4.52 - \log SiO_2) - 273.15$	Fournier (1977).
2	SiO_2 (α Christobalite)	$t = 1000 / (4.78 - \log SiO_2) - 273.15$	Fournier (1977).
3	SiO_2 (βChristobalite)	$t = 781 / (4.51 - \log SiO_2) - 273.15$	Fournier (1977).
4	SiO_2 (Chalcedony)	$t = 1032 / (4.69 - \log SiO_2) - 273.15$	Fournier (1977).
5	SiO_2 (Quartz)	$t = 1309 / (5.19 - \log SiO_2) - 273.15$	Fournier (1977).
6	SiO_2 (Quartz-steam loss)	$t = 1522 / (5.75 - \log SiO_2) - 273.15$	Fournier (1977).
7	Na/K	$t = 933/(0.933 + \log Na/K) - 273.15$	Arnórsson et al. (1983).
8	Na/K	$t = 1319/(1.699 + \log Na/K) - 273.15$	Arnórsson et al. (1983).
9	Na/K	$t = 777/(0.70 + \log Na/K) - 273.15$	Arnórsson et al. (1983).
10	Na/K	$t = 856/(0.857 + \log Na/K) - 273.15$	Truesdell (1976).
11	K/Mg	$t = 4410/(13.95 - \log K^2/Mg) - 273.15$	Giggenbach et al. (1983).
12	Na-K-Ca (mmol)	$t = 1647/(\log Na/K + \beta \log \sqrt{a}/Na + 2.24) - 273.15$	Fournier and Truesdell (1973).
13	Na-K-Ca (R) (Mg correction)	$R = (Mg/Mg+Ca+K) \times 100$	Fournier and Potter (1979).
14	Li/Mg	$t = 2200/(5.470 - \log (Li/Mg^{0.5})) - 273.15$	Kharaka and Mariner (1989).
15	Na/Li	$t = 1590/(0.779 + \log (Na/Li)) - 273.15$	Kharaka et al. (1982).
16	Na/Li (mmol) Cl < 0.3	$t = 1000/(0.389 + \log (Na/Li)) - 273.15$	Fouillac and Michard (1981).
17	Na-Li (mmol) Cl > 0.3	$t = 1195/(0.130 + \log (Na/Li^{0.5})) - 273.15$	Fouillac and Michard (1981).

Table 4. Estimated temperatures by various geothermometers.

Sample	Temperature (°C)	SiO_2 amorphous	SiO_2 α-christobalite	SiO_2 B-christobalite	SiO_2 chalcedony	SiO_2 quartz	SiO_2 quartz-steam loss
2	30.6	45	123	74	151	173	163
4	63	7	80	32	104	131	128
5	183	52	131	81	159	180	168
17	29.1	6	80	31	103	130	127
21	28	-11	59	12	80	109	109
22	31	-20	49	3	70	100	101
30	16.7	-14	56	9	77	107	107
38	213	121	206	156	243	251	224
109	57	32	109	59	135	159	151

Table 5. Estimated temperatures by various geothermometers.

Sample	Temperature (°C)	(7) Na/K	(8) Na/K	(9) Na/K	(10) Na/K	(11) K/Mg	(12) Na-K-Ca	(13) Na-K-Ca-Mg	(14) Mg/Li	(15) Na/Li	(16) Na/Li	(17) Na/Li
2	30.6	176	181	231	211	42	187	29	125	289	183	169
4	63	30	41	99	90	21	129	92	108	116	17	29
5	183	86	96	152	140	13	169	143	172	188	83	87
17	29.1	137	144	198	182	51	142	83	52	183	78	83
21	28	85	95	151	139	62	120	29	18	114	15	27
22	31	87	97	153	141	60	122	42	10	92	-4	9
30	16.7	228	228	273	248	52	205		80	269	163	153
38	213	197	200	249	227	5	227	209	220	283	178	165
109	57	76	86	143	132	41	143	34	81	146	44	53

were investigated by Tarcan (2004) in point of scaling tendencies and geothermometer applications. In this study, scaling tendencies and geothermometer applications of 10 waters in the study area were

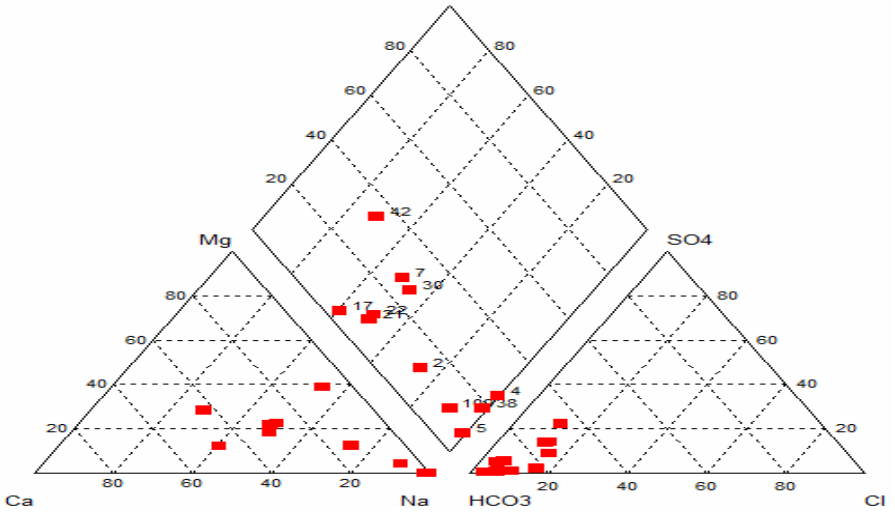

Figure 9. Distribution of thermal waters from the study area in a Piper diagram.

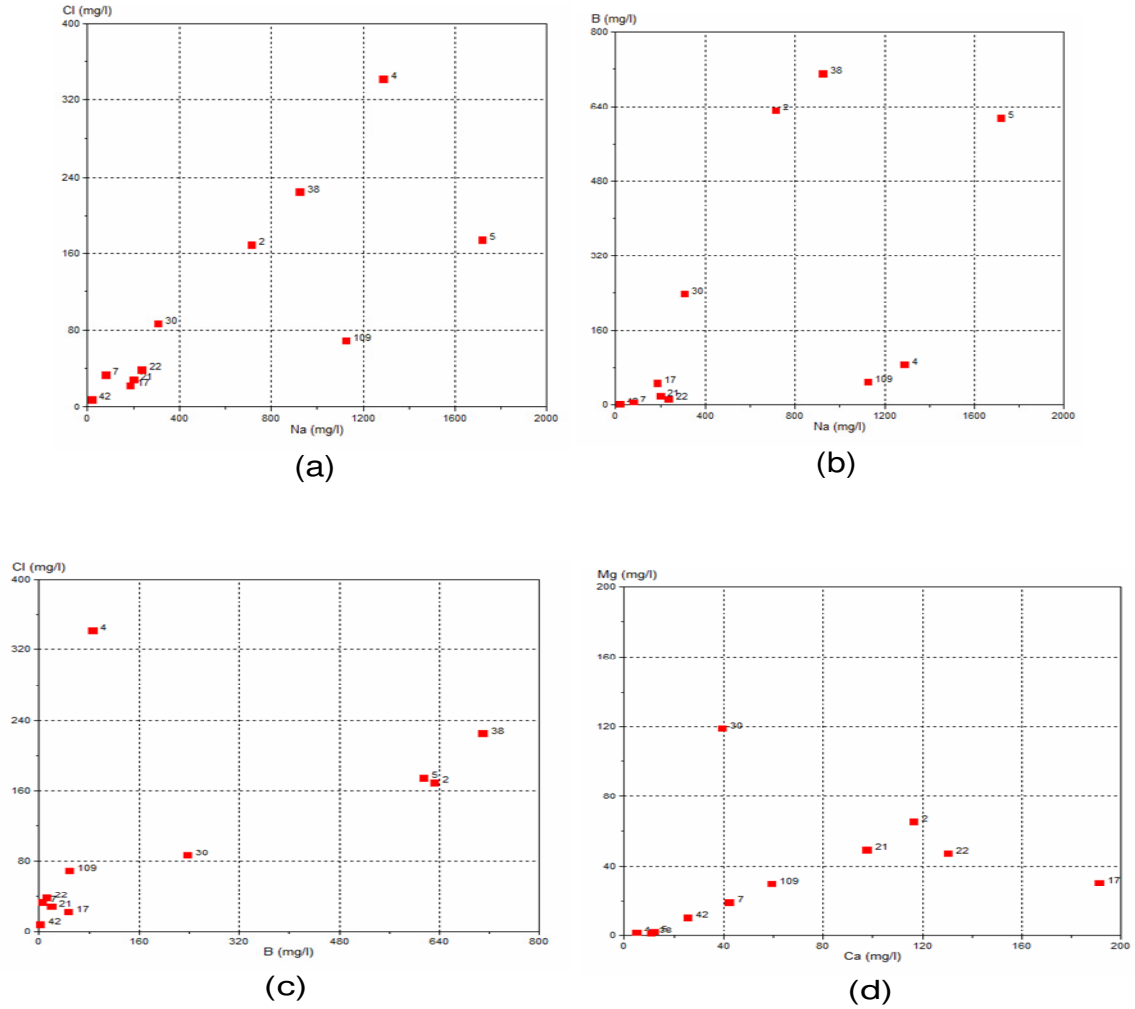

evaluated. Also very high boron concentrations were determined in thermal waters of Horzumsazdere spa and

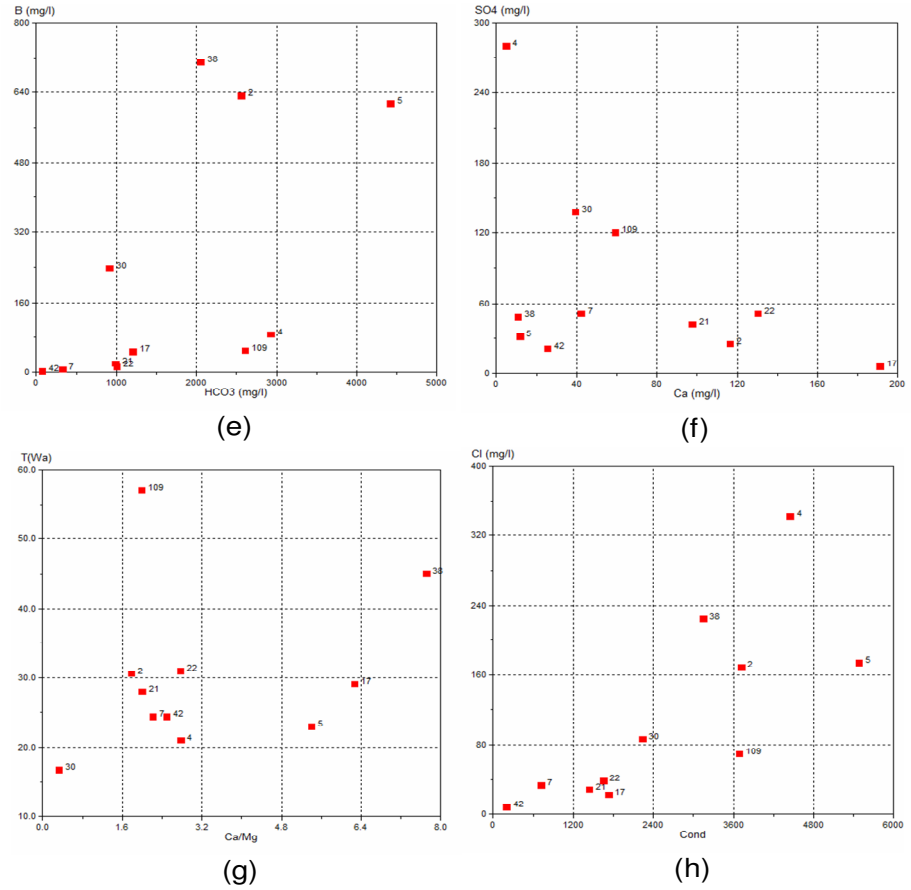

Figure 10. Scatter diagrams to show relationship between some parameters: (a) Cl-Na, (b) B-Na, (c) Cl-B, (d) Mg-Ca, (e) B-HCO_3, (f) SO4-

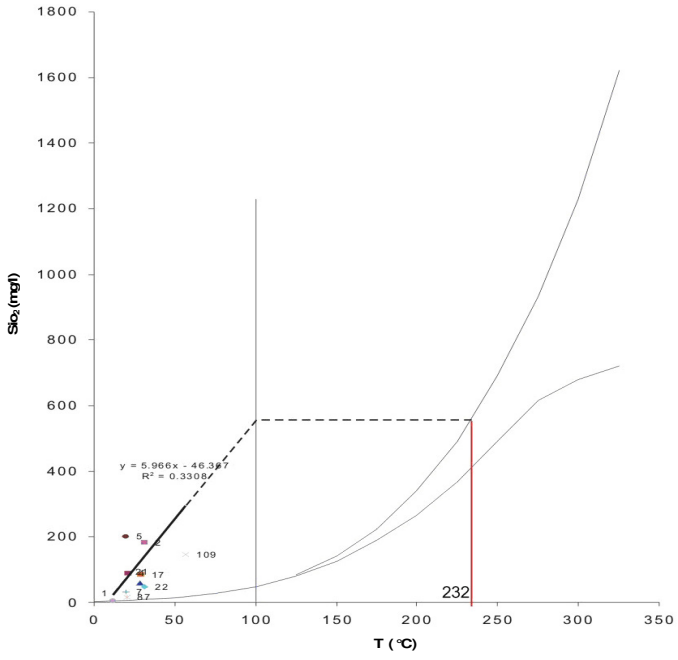

Figure 11. Silica enthalpy model for geothermal area.

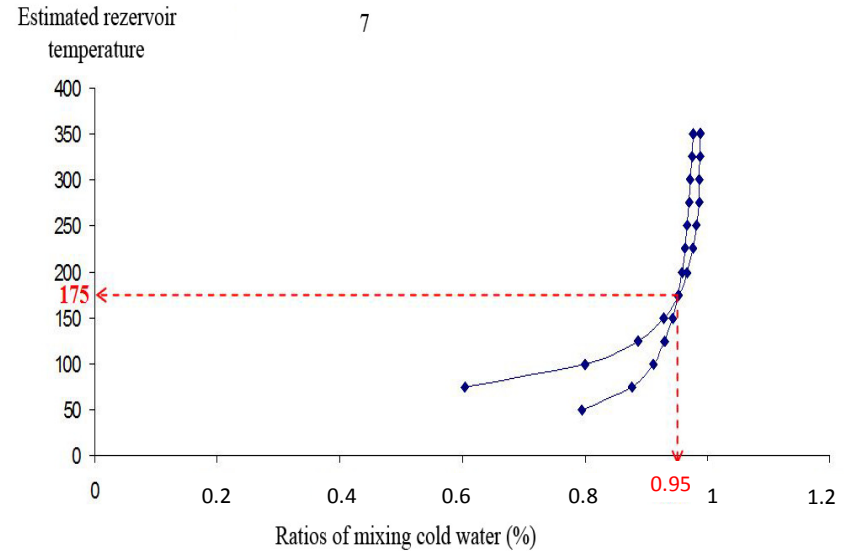
Estimated rezervoir temperature
7
400
350
300
250
200
175
150
100
50
0
0
0.2
0.4
0.6
0.8
0.95
1
1.2
Ratios of mixing cold water (%)

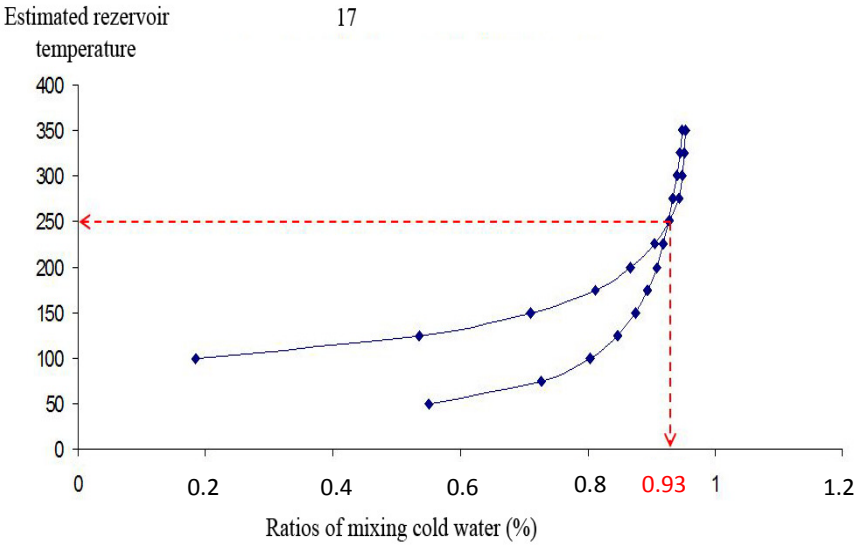
Estimated rezervoir temperature
17
400
350
300
250
200
150
100
50
0
0
0.2
0.4
0.6
0.8
0.93
1
1.2
Ratios of mixing cold water (%)

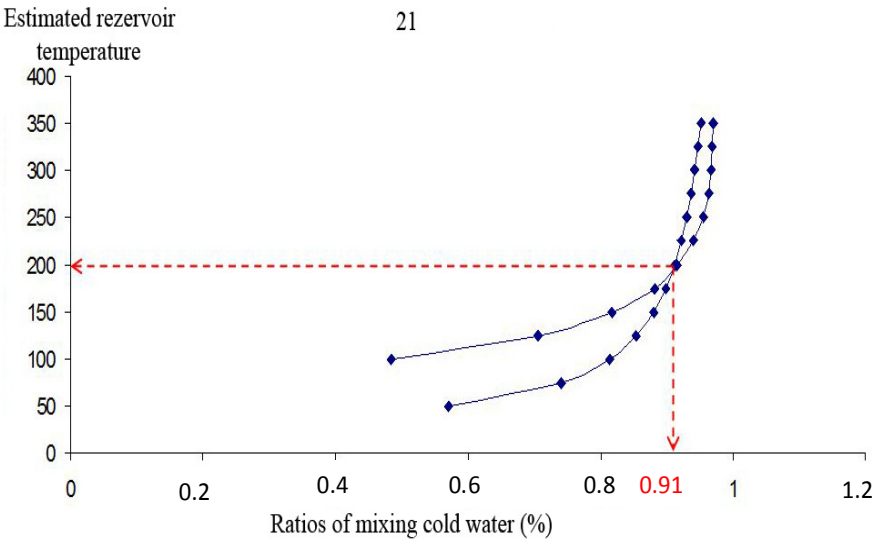
Estimated rezervoir temperature
21
400
350
300
250
200
150
100
50
0
0
0.2
0.4
0.6
0.8
0.91
1
1.2
Ratios of mixing cold water (%)

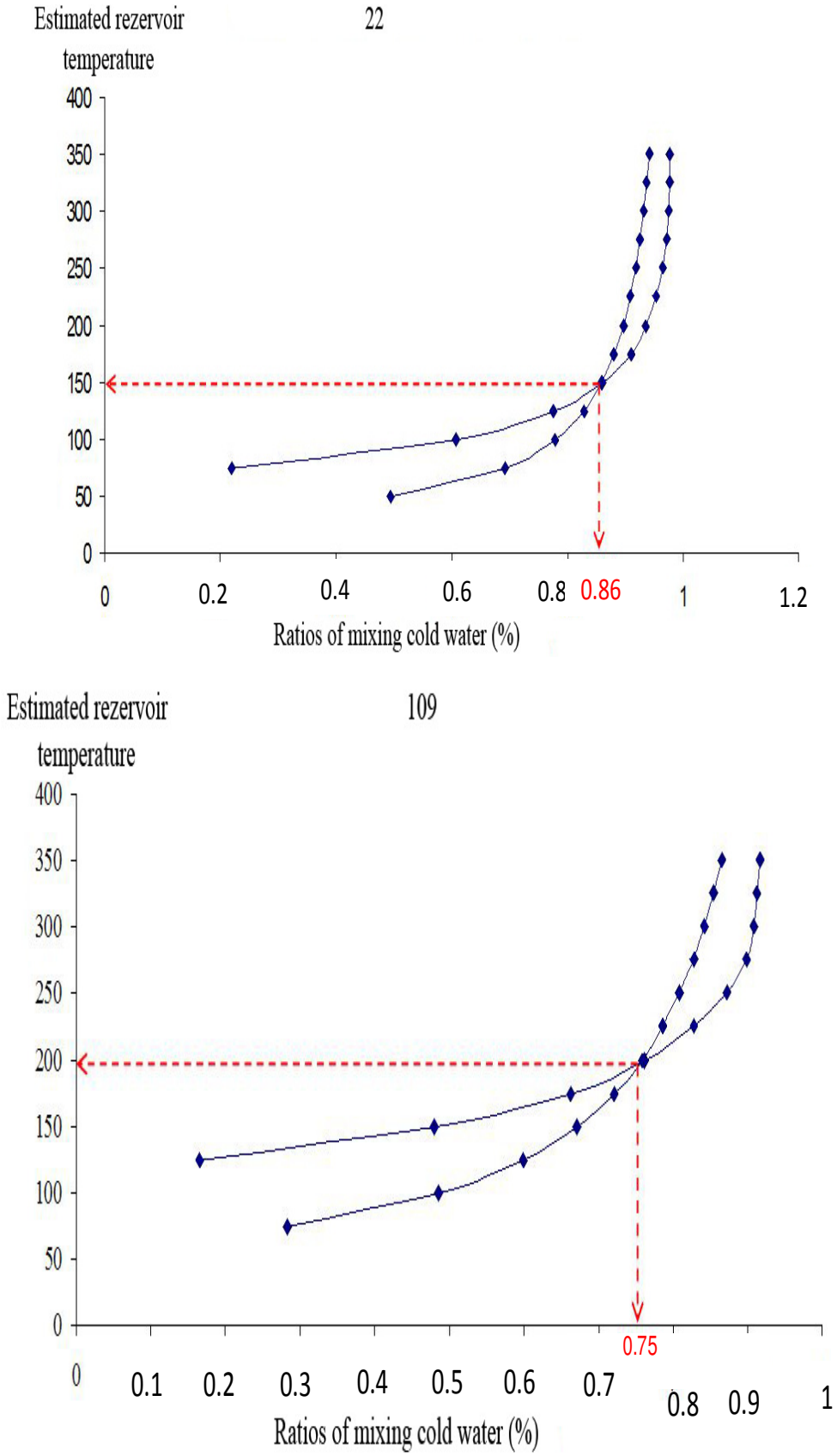

Figure 12. Silica mixing models for some thermal waters (number 7, 17, 21, 22 and 109) in the area.

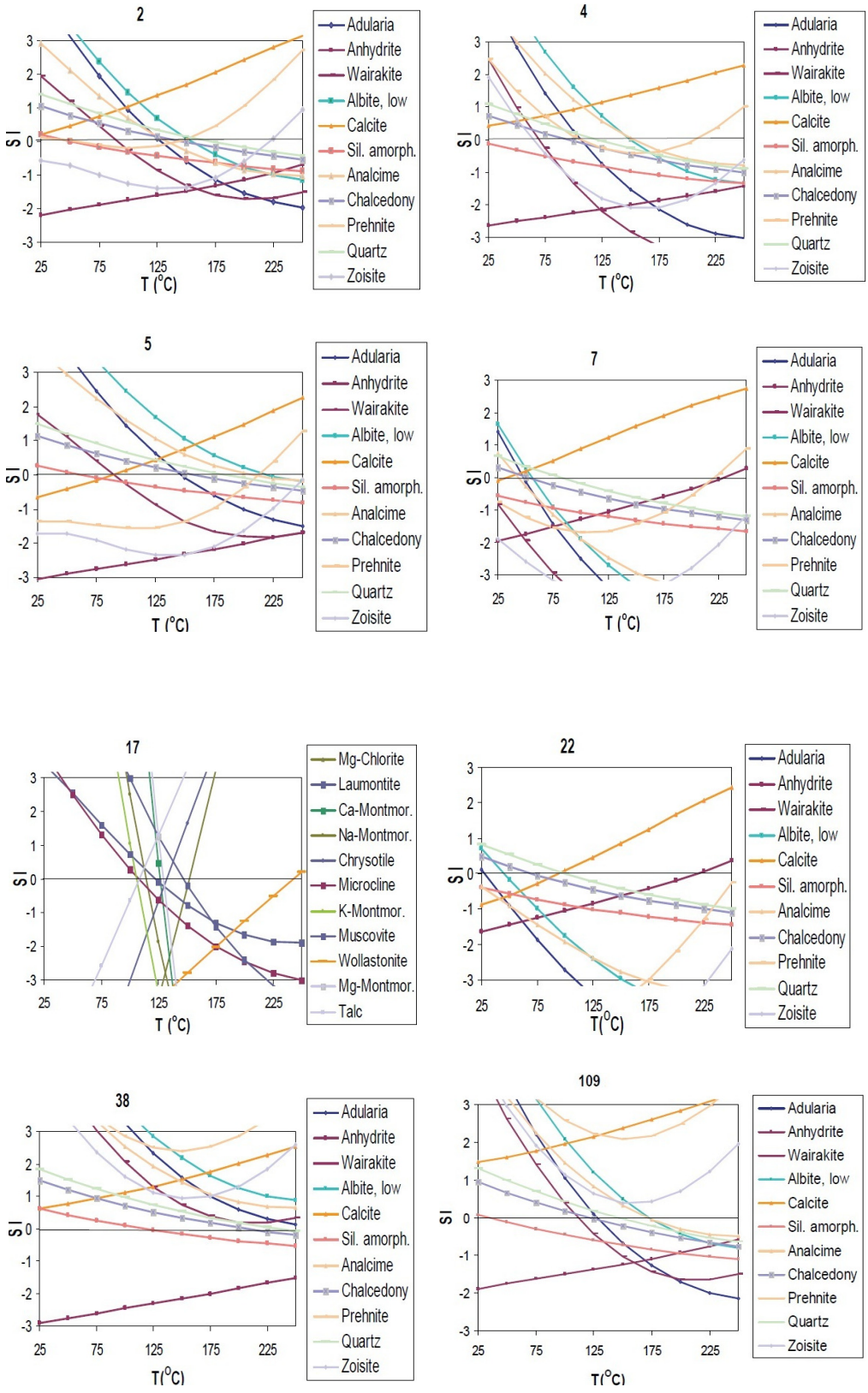

Figure 13. Changes in the state of calcite saturation in waters from selected geothermal wells (number 2, 4, 5, 7, 17, 22, 38 and 109) in the study area upon conductive cooling.

Table 6. Saturation index of thermal waters from spa and wells at outlet temperature for various mineral phases. *(+): oversaturated and (-): undersaturated.

Phas	Formula	Saturation index according to sample numbers													
		2	4	5	7	17	21	22	30	38	42	109	An.	m.	SI*
Albite	$NaAlSi_3O_8$	2.7	3.6	3.8	-0.3	0.6	0.2	-0.9	0.7	4.2	-0.7	1.9	15.7	1.4	+
Alunite	$KAl_3(SO_4)_2(OH)_6$	0.4	-2.4	3.6	-3.4	0.0	-1.2	-0.3	-8.9	-6.8	-4.7	-8.3	-31.9	-2.9	-
Anhydrite	$CaSO_4$	-2.6	-3.0	-3.6	-2.3	-2.9	-2.3	-2.1	-2.3	-3.3	-2.8	-2.1	-29.2	-2.7	-
Anorthite	$CaAl_2Si_2O_8$	-0.2	0.2	-0.6	-2.0	-1.7	-2.3	-3.8	-3.1	1.2	-0.6	0.3	-12.5	-1.1	-
Aragonite	$CaCO_3$	0.2	0.2	-0.9	-0.2	-0.3	-0.2	-0.6	1.0	0.6	-0.3	1.5	1.1	0.1	+
Barite	$BaSO_4$	0.1	1.4	0.4	0.2	-0.7	0.0	0.4	0.3	0.8	-0.5	0.3	2.7	0.2	+
Calcite	$CaCO_3$	0.4	0.4	-0.8	0.0	-0.2	0.0	-0.4	1.1	0.8	-0.2	1.6	2.6	0.2	+
Celestite	$SrSO_4$	-2.6	-2.1	-2.6	-2.4	-3.0	-2.5	-2.5	-2.0	-2.7	-3.1	-2.1	-27.6	-2.5	-
Chalcedony	SiO_2	1.0	0.8	1.1	0.3	0.7	0.5	0.4	0.6	1.2	0.0	0.6	7.1	0.6	+
Chlorite(14A)	$Mg_5Al_2Si_3O_{10}(OH)_8$	-3.7	0.2	-13.8	-2.8	-11.4	-7.2	-12.8	6.3	4.5	2.3	10.3	-28.1	-2.6	-
Chrysotile	$Mg_3Si_2O_5(OH)_4$	-6.0	-3.4	-12.7	-4.7	-10.6	-7.6	-10.7	2.8	-0.2	-2.3	3.4	-52.0	-4.7	-
CO_2(g)	CO_2	-0.2	-1.8	0.2	-1.8	0.0	-0.6	0.0	-2.5	-1.6	-3.1	-1.4	-12.7	-1.2	-
Dolomite	$CaMg(CO_3)_2$	0.9	0.6	-2.0	0.0	-0.7	0.0	-0.9	3.0	1.2	-0.4	3.5	5.2	0.5	+
Gibbsite	$Al(OH)_3$	1.9	1.8	2.6	1.3	1.8	1.4	1.1	-0.2	0.8	8.3	6.8	27.5	2.5	+
Goethite	FeOOH	3.3	10.0	7.2	7.3	5.3	5.6	3.7	6.2	7.6	-2.6	-2.1	51.5	4.7	+
Gypsum	$CaSO_4{:}2H_2O$	-2.4	-2.8	-3.4	-2.1	-2.7	-2.1	-1.9	-2.0	-3.2	-23.9	-23.8	-70.2	-6.4	-
Hausmannite	Mn_3O_4	-17.3	-11.3	-19.4	-16.5	-20.2	-15.5	-21.1	-14.9	-7.3	18.6	17.8	-107.0	-9.7	-
Hematite	Fe_2O_3	9.0	21.7	16.2	16.6	13.0	13.3	9.8	13.9	18.6	0.5	4.2	136.7	12.4	+
İllite	$K0.6Mg0.25Al_2.3Si_3.5O_{10}(OH)_2$	6.9	6.9	8.3	3.2	4.7	3.5	1.9	2.6	6.8	3.7	3.5	52.0	4.7	+
K-feldspar	$KAlSi_3O_8$	3.9	4.2	4.7	0.9	1.7	1.0	-0.1	2.3	5.3	0.9	2.4	27.3	2.5	+
K-mica	$KAl_3Si_3O10(OH)_2$	13.3	13.4	15.5	9.1	11.0	9.3	7.8	7.5	12.6	9.9	8.8	118.2	10.7	+
Kaolinite	$Al_2Si_2O_5(OH)_4$	7.3	6.9	9.1	4.8	6.7	5.4	4.6	2.6	5.7	5.1	3.4	61.5	5.6	+
Manganite	MnOOH	-7.7	-4.4	-7.8	-6.7	-8.7	-6.9	-9.2	-5.1	-5.0	-4.2	-4.5	-70.2	-6.4	-
Quartz	SiO_2	1.4	1.2	1.6	0.7	1.1	0.9	0.8	1.1	1.6	0.4	0.9	11.7	1.1	+
Rhodochrosite	$MnCO_3$	-0.1	0.0	0.3	-1.5	-0.4	0.3	-0.8	-1.7	-0.2	-0.9	0.5	-4.5	-0.4	-
Sepiolite	$Mg_2Si_3O_7.5OH{:}3H_2O$	-2.8	-1.0	-6.8	-2.9	-6.3	-4.5	-6.9	3.0	1.1	-1.7	2.0	-27.0	-2.5	-
Siderite	$FeCO_3$	-2.8	0.9	1.8	-1.1	0.0	-0.8	-1.6	-3.7	-1.6	-1.9	-2.3	-13.3	-1.2	-
SiO_2(a)	SiO_2	0.2	-0.1	0.3	-0.6	-0.2	-0.3	-0.4	-0.3	0.5	-0.9	-0.2	-1.9	-0.2	-
Strontianite	$SrCO_3$	-1.1	-0.2	-1.3	-1.5	-1.8	-1.7	-2.3	0.0	-0.2	-2.0	0.2	-12.0	-1.1	-
Talc	$Mg_3Si_4O_{10}(OH)_2$	-0.3	1.8	-6.8	-0.5	-5.5	-2.8	-6.2	7.6	6.3	1.4	8.7	3.6	0.3	+
Witherite	$BaCO_3$	-2.4	-0.8	-2.3	-3.0	-3.4	-3.3	-3.4	-2.0	-0.5	-3.4	-1.1	-25.5	-2.3	-

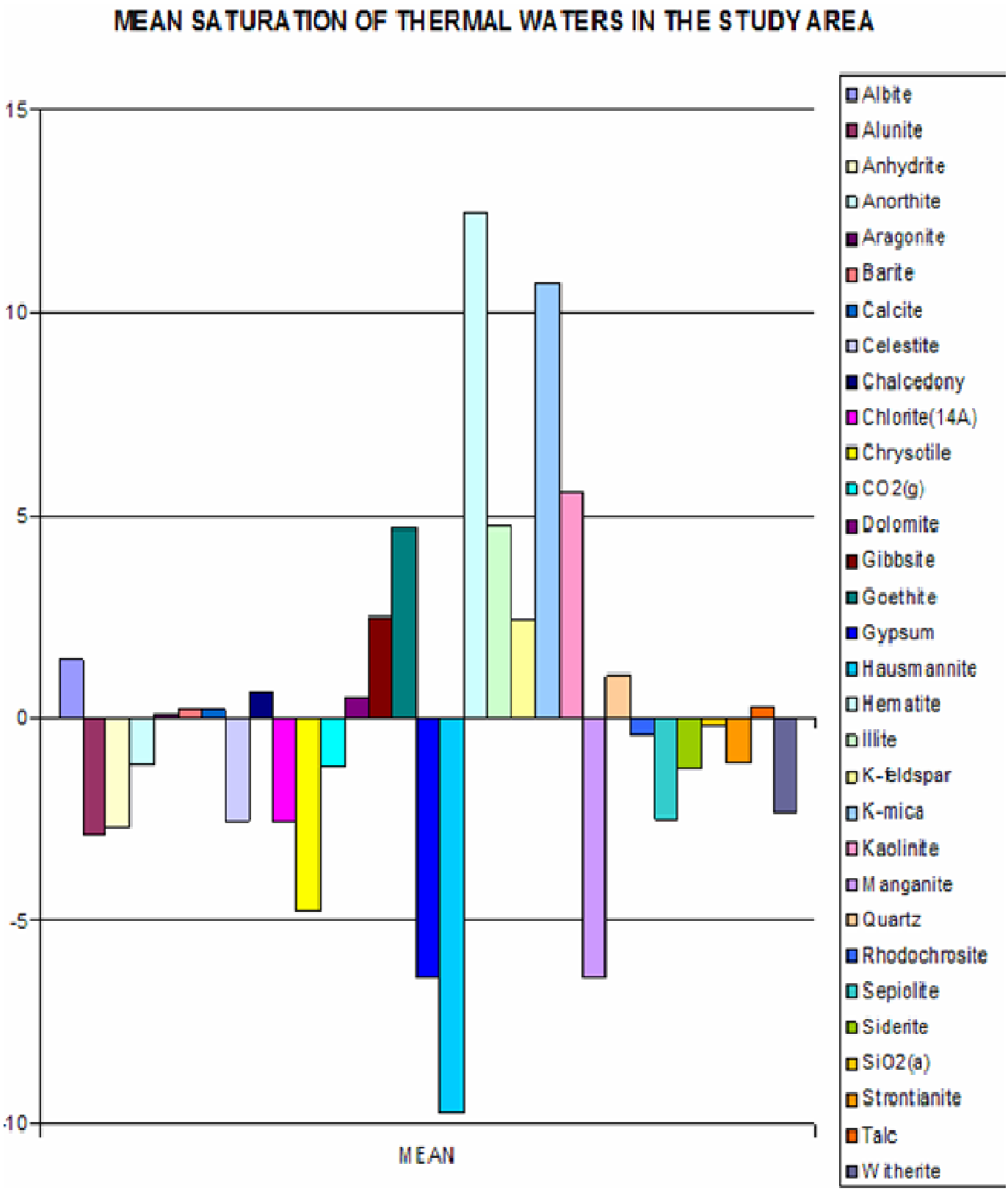

Figure 14. Stick diagram of mean saturation index for various minerals in the study area.

AK-2 well. In the study area a conceptual geothermal model was proposed (Figure-4).

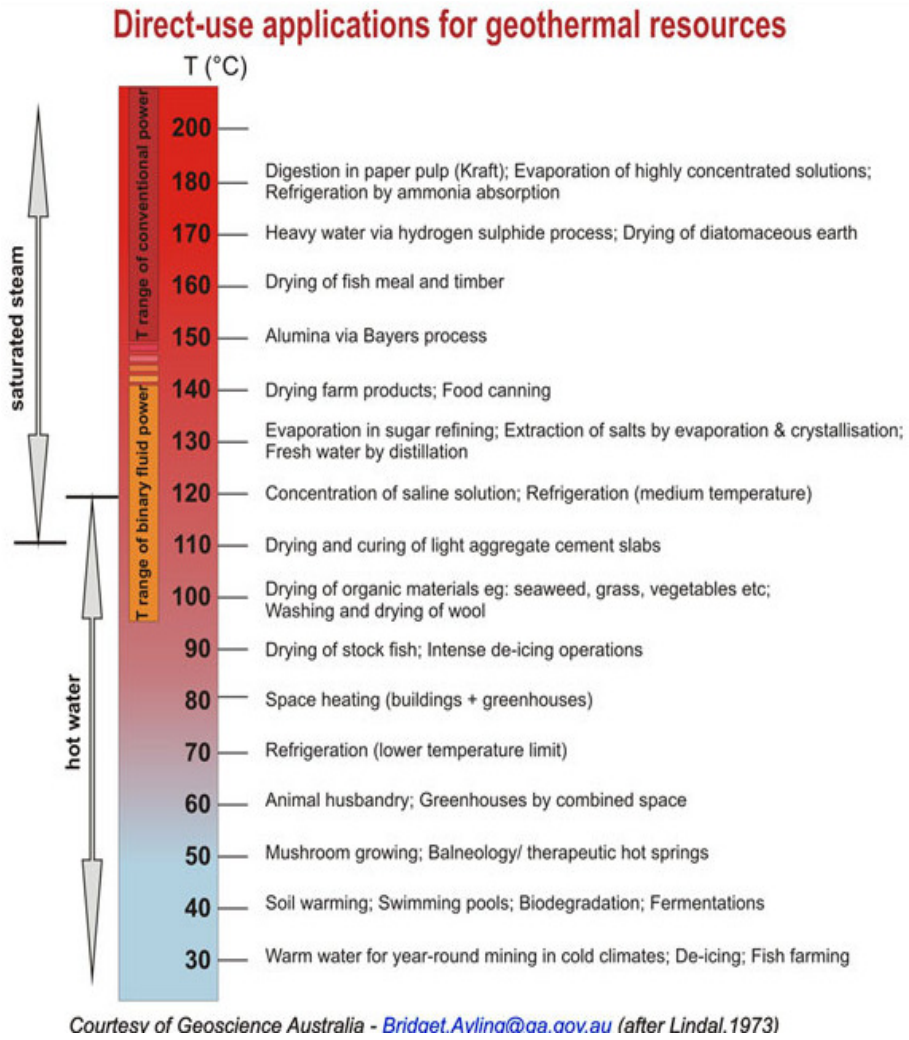

Figure 15. Modified Lindal diagram (1973).

ACKNOWLEDGEMENTS

The authors acknowledge the financial support of

TÜBİTAK Research Fund (106Y160) and thank the editor and the anonymous reviewers for many comments and suggestions.

REFERENCES

Arnórsson S, Gunnlaugsson E, Svavarsson H (1983). The chemistry of geothermal waters in İceland. İİİ. Chemical geothermometry in geothermal investigations. Geochimica et Cosmoschimica, Acta. (47): 567-577.

Bülbül A (2009). Hyrogeological and Hydrogeochemical İnvestigation of hot and cold water systems of Alasehir (Manisa). Phd. Thesis, DEU İnstitue of Sciences, İZMİR (In Turkish).

Calmbach L (1997). AquaChem Computer Code-Version 3.7.42, waterloo hydrogeologic. Ontario, Canada, N2L 3L3.

Çiftçi NB, Bozkurt E (2009). Structural evolution of the Gediz Graben, SW Turkey: temporal and spatial variation of the graben basin. Basin Research 10. 1111/j. pp.1365-2117.

Dewey JF, Sengör AMC (1979). Aegean and surrounding regions: complex multiplate and continuum tectonics in a convergent zone. Geological Society of America Bulletin, Pt. İ. 90: 84-92.

Fouillac C, Michard G (1981). Sodium/Lithium ratio in water applied to the geothermometry of geothermal waters. *Geothermics*. 10: 55-70.

Fournier RO, Potter RW (1979). Magnesium Correction to the Na-K-Ca Chemical Geothermometer. Geochimica et Cosmochimica Acta. 43: 1543-1550.

Fournier RO (1977). Chemical geotermometers and mixing models for geothermal systems. İn: Proceedings of the Symposium on Geothermal Energy, Centro Scientific Programme, Ankara. 199-210.

Fournier RO, Truesdell AH (1973). An Empirical Na-K-Ca Geothermometer for Natural Waters. Geochimica et Cosmochimica Acta. 37: 1255-1275.

Gemici Ü, Tarcan G (2002). Distribution of boron in thermal waters of western Anatolia, Turkey and examples on their environmental impacts. Environ. Geol. 43: 87-98.

Giggenbach WF (1988). Geothermal Solute Equilibria. Derivation of Na-K-Mg-Ca Geoindicators. Geochim. et Cosmochim Acta. 52: 2749-2765.

Giggenbach WF, Gonantini R, Jangi BL, Truesdell AH (1983). İsotopic and Chemical Composition of Parbati Valley Geothermal Discharges, NW Himalaya, İndiana. Geothermics. 12: 199-222.

Gökgöz A (1998). Geochemistry of the Kizildere-Tekkehamam-Buldan-Pamukkale Geothermal Fields, Turkey, The United Nations University, Geothermal Training Programme, Orkustofnun, Reykjavik, İceland.

Karahan Ç, Bakraç S, Dünya H (2003). Evaluation of the Alasehir-Kavaklidere-Göbekli Drill (KG-1). Drill Symposium 2003, MTA, İzmir.

Kharaka YK, Mariner RH (1989). Chemical Geothermometers and their Application to formation waters from sedimentary basins. İn: N.D. Näser and T.H. McCulloh (Eds.). Thermal History of Sedimentary Basins Methods and Case Histories. Springer Verlag.pp. 99-117.

Kharaka YK, Lico MS, Law LM (1982). Chemical geothermometers applied to formation waters, Gulf of Mexico and California Basins. Am. Assoc. Petrol. Geol. Bull.pp. 66-558.

Lindal B (1973). Industrial and other applications of geothermal energy, In Geothermal Energy: Review of Research and Development, Paris, UNESCO, LC No. 72-97138. pp.135-148.

Parkhurst DL, Appelo CAJ (1999). User's guide to PHREEQC (version 2)-A computer program for speciation, batch-reaction, one-dimensional transport, and inverse geochemical calculations: U.S. Geological Survey Water-Resources İnvestigations Report. 99 (312): 4259.

Purvis M, Robertson A (2005). Sedimentation of the Neogene–Recent Alasehir (Gediz) continental graben system used to test alternative tectonic models for western (Aegean) Turkey. Sedimentary Geol.173: 373-408.

Reed M, Spycher N (1984). Calculation of pH and mineral equilibria in hydrothermal waters with application to geothermometry and studies of boiling and dilution. *Geochim. Cosmochim.* Acta. 48: 1479-1492.

Seyitoğlu G, Tekeli O, Çemen İ, Sen S, İsik V (2002). The role of the flexural rotation/rolling hinge model in the tectonic evolution of the Alasehir graben, western Turkey. Geological Magazine,139: 15-26.

Seyitoğlu G, Scott B (1996a). The age of the Alasehir graben (west Turkey) ad its tectonic implications. Geological Magazine,139: 15-26.

Tarcan G (2004). Mineral saturation and scaling tendencies of waters discharged from wells (>150^{o}C) in geotermal areas of Turkey. J. volcano. geotermal research. 142: 263-283.

Truesdell AH (1976). Summary of section İİİ geochemical techniques in exploration. Proceedings, Second United Nations Symposium on the Development and Use of Geothermal Resources. San Francisco, 1975. Washington D. C., U. S. Government Printing Office. 1.